1

Sensing of Blood Pressure Increase by Transient Receptor Potential Vanilloid 1 Receptors on Baroreceptors

Hao Sun, De-Pei Li, Shao-Rui Chen, Walter N. Hittelman, Hui-Lin Pan

Department of Anesthesiology and Perioperative Medicine (HS, SRC, HLP)

Department of Critical Care (DPL)

Department of Experimental Therapeutics (WNH)

The University of Texas M. D. Anderson Cancer Center

Houston, TX 77030

Running Title: TRPV1 and cardiovascular regulation

Number of text pages: 30

Number of tables: 0;

Number of figures: 8;

Number of references: 40

Number of words in Abstract: 244

Number of words in Introduction: 566

Number of words in Discussion: 1184

List of Abbreviations: ABP: arterial blood pressure; HR: heart rate; IB$_4$: *Griffonia simplicifolia* isolectin B$_4$; MAP: mean arterial pressure; RSNA: renal sympathetic nerve activity; RTX: resiniferatoxin; PE: phenylephrine; SNP: sodium nitroprusside; TRPV1: transient receptor potential vanilloid type 1; NG: nodose ganglion; NTS: nucleus tractus solitarius

Address for correspondence:

Hui-Lin Pan, M.D., Ph.D.

Division of Anesthesiology and Perioperative Medicine, Unit 110

The University of Texas M. D. Anderson Cancer Center

1515 Holcombe Blvd., Houston, TX 77030

Tel: (713) 563-5838; Fax: (713) 794-4590

E-mail: huilinpan@mdanderson.org

Abstract

The arterial baroreceptor is critically involved in the autonomic regulation of homoeostasis. The transient receptor potential vanilloid 1 (TRPV1) receptor is expressed on both somatic and visceral sensory neurons. Here we examined the TRPV1 innervation of baroreceptive pathways and its functional significance in the baroreflex. Resiniferatoxin (RTX), an ultrapotent analogue of capsaicin, was used to ablate TRPV1-expressing afferent neurons and fibers in adult rats. Immunofluorescence labeling revealed that TRPV1-immunoreactivity was present on nerve fibers and terminals in the adventitia of the ascending aorta and aortic arch, the nodose ganglion neurons, and afferent fibers in the solitary tract of the brainstem. RTX treatment eliminated TRPV1-immunoreactivities in the aorta, nodose ganglion, and solitary tract. Renal sympathetic nerve activity, blood pressure, and heart rate were recorded in anesthetized rats. The baroreflex was triggered by lowering and raising blood pressure through intravenous infusion of sodium nitroprusside and phenylephrine, respectively. Inhibition of sympathetic nerve activity and heart rate by the phenylephrine-induced increase in blood pressure was largely impaired in RTX-treated rats. The maximum gain of the baroreflex function was significantly lower in RTX-treated than vehicle-treated rats. Furthermore, blocking of TRPV1 receptors significantly blunted the baroreflex and decreased the maximum gain of baroreflex function in the high blood pressure range. Our findings provide important new information that TRPV1 is expressed along the entire baroreceptive afferent pathway. TRPV1 expressed on baroreceptive nerve endings can function as mechanoreceptors to detect the increase in blood pressure and maintain the homoeostasis.

Introduction

The arterial baroreflex is the primary feedback mechanism that regulates systemic blood pressure and cardiovascular homeostasis. The baroreceptors located in the aortic arch detect fluctuations in blood pressure and convey this sensory information to the nucleus tractus solitarius (NTS) through the aortic depressor nerve and nodose ganglion (NG) (Tranum-Jensen, 1975; Krauhs, 1979; Kunze and Andresen, 1991). The baroreceptive afferents are divided into myelinated (Aδ-fiber) and unmyelinated (C-fiber) nerve fibers based on the presence of myelination and conduction velocity of the nerve axon (Krauhs, 1979). In general, Aδ-fibers have lower pressure thresholds, higher firing rates, and more regular discharges than C-fibers (Thoren et al., 1999). Anodal blocking of Aδ-fibers results in a significant decrease in baroreflex sensitivity without changing the baseline levels of arterial blood pressure (ABP) (Seagard et al., 1993). On the other hand, anesthetic blockade of C-fibers leads to a decrease in baroreflex sensitivity and significantly elevates baseline ABP (Seagard et al., 1993). This suggests that Aδ- and C-fiber baroreceptive nerves contribute differentially to ABP regulation.

Primary sensory neurons in the dorsal root ganglion (DRG) and NG and their associated nerve fibers are highly heterogenous because they express diverse ion channels and receptors. Based on the expression of neurotrophic factor receptors regulating the neuronal survival in adulthood, small-diameter sensory neurons have been classified into two broad groups (McMahon et al., 1994; Averill et al., 1995). One class expresses the TrkA receptor for nerve growth factor and contains neuropeptides such as substance P and calcitonin gene-related peptide. The other class possesses cell surface glyco-conjugates that can be identified by their

binding with the *Griffonia simplicifolia* isolectin B_4 (IB_4) (Wang et al., 1994; Bennett et al., 1998). IB_4-positive neurons express receptors for glial cell line-derived neurotrophic factor and are relatively 'peptide poor', but most of them express P2X3 and transient receptor potential vanilloid 1 (TRPV1) receptors (Bradbury et al., 1998; Guo et al., 1999). However, the phenotypes and functional significance of baroreceptive afferent nerves and neurons are not well understood.

A key membrane channel protein associated with small sensory neurons is the TRPV1 receptor, which is a non-selective cation channel activated typically by capsaicin, noxious heat, and protons (Caterina et al., 1999). In addition to being present in some DRG neurons and cutaneous afferent nerves, TRPV1 is expressed in the NG (Michael and Priestley, 1999; Patterson et al., 2003) and visceral afferent fibers (Birder et al., 2002; Zahner et al., 2003; Pan and Chen, 2004; Rong et al., 2004). Stimulation of TRPV1 afferent terminals can increase glutamate release to NTS neurons (Doyle et al., 2002; Jin et al., 2004). However, the distribution of TRPV1 along the baroreceptive pathway has not been systematically determined. Therefore, in this study, we examined the presence of TRPV1-expressing neurons and nerve fibers in the baroreceptive pathway. Resiniferatoxin (RTX) is an ultra-potent analogue of capsaicin and can ablate TRPV1-expressing primary afferent nerves and neurons upon systemic administration in adult rats (Pan et al., 2003). In this study, we used RTX to determine the contributions of TRPV1 receptors and TRPV1-expressing afferent neurons to the baroreflex function. Our study provides new histologic and functional evidence about the important role of TRPV1 on baroreceptive afferent fibers in sensing changes in blood pressure and in regulating cardiovascular homeostasis.

Methods

Animals and RTX Treatment

The surgical procedures and experimental protocols used in this study were approved by the Institutional Animal Care and Use Committee of The University of Texas M. D. Anderson Cancer Center and were in accordance with the National Institutes of Health guidelines on the ethical use of animals. Male Sprague-Dawley rats (9 weeks old; Harlan, Indianapolis, IN) were used in this study. Rats in the RTX treatment group received a single intraperitoneal injection of RTX (200 µg/kg; LC Laboratories, Woburn, MA) under isoflurane (2% in O_2) anesthesia. RTX was dissolved in a mixture of 10% Tween 80 and 10% ethanol in saline (Pan et al., 2003; Zahner et al., 2003). Rats in the control group received an intraperitoneal injection of vehicle alone.

To determine the effect of RTX treatment on thermal nociception, we measured the thermal sensitivity of the rat hindpaw to a noxious heat stimulus by placing each rat in an individual Plexiglas enclosure on the transparent glass surface maintained at a constant 30°C. After a 30-min acclimation period, the heat-emitting projector lamp of a thermal testing apparatus (IITC Life Sciences Inc., Woodland Hills, CA) was activated, and the beam was focused directly onto the plantar surface of the hindpaw of each rat. A built-in digital timer was used to record the paw withdrawal latency. The mean value of the withdrawal latency on 2 or 3 consecutive trials was calculated. A cutoff of 30 s was used to avoid potential tissue damage.

Immunofluorescence Labeling of TRPV1 in the Aorta

Immunofluorescence labeling was performed on four vehicle- and four RTX-treated rats (4 weeks after treatment).   Under deep anesthesia with sodium pentobarbital (60 mg/kg, i.p.), rats were perfused intracardially with 4% paraformaldehyde in 0.1 M phosphate-buffered saline (PBS) and 10% sucrose in PBS (pH 7.4).   The ascending aorta and aortic arch, brainstem, DRG, and NG were quickly removed and cryoprotected in 30% sucrose in PBS for 48 hr at 4 °C.

The aortic tissues were cut into 40-μm-thick sections and collected free-floating in 0.1 M PBS.   To examine the presence of TRPV1-expressing nerve fibers and terminals, the aortic tissue sections were labeled with the TRPV1 primary antibody (guinea pig anti-TRPV1, dilution 1:1000, Neuromics, Minneapolis, MN) and secondary antibody (Alexa Fluor-488 conjugated goat anti-guinea pig IgG, dilution 1:200, Molecular Probes, Eugene, OR).   The specificity of this particular TRPV1 primary antibody has been extensively characterized in our previous studies (Pan et al., 2003; Chen and Pan, 2006; Zhou et al., 2009).   To determine whether TRPV1 is present on myelinated afferent nerves innervating the aorta, we also labeled sections with NF200, a marker for the myelinated nerve fibers (Perry et al., 1991).   Briefly, sections were rinsed in TBS, blocked with 4% normal goat serum, and incubated with a mixture of primary antibodies (guinea pig anti-TRPV1, dilution 1:1000, Neuromics; and rabbit anti-NF200, dilution 1:100, Chemicon, Temecula, CA) for 2 hr at room temperature and overnight at 4 °C. Subsequently, sections were rinsed and incubated with a mixture of secondary antibodies (Alexa Fluor-488 conjugated goat anti-guinea pig IgG, dilution 1:200; and Alexa Fluor-594 conjugated goat anti-rabbit IgG, dilution, 1:200; Molecular Probes) for 2 hr at room temperature.   The

negative control was done by omitting the primary antibodies.

The sections were examined on a laser scanning confocal microscope (LSM 510, Zeiss, Jena, Germany), and areas of interest were photodocumented.   To better visualize the nerve fiber track, which would be missed in the single-plane image, we reconstructed images in the aortic region from Z-stack and obtained the maximal projection image to depict the profile of nerve fibers and terminals.

Double Fluorescence Labeling of TRPV1 and IB$_4$ in NG, DRG, and NTS

We next performed double fluorescence labeling of TRPV1 and IB$_4$, a marker for unmyelinated afferent neurons and fibers in the NG, DRG (at the L5 and L6 level), and NTS (Pan et al., 2003; Wu et al., 2004; Chen and Pan, 2006).   The NG and DRG tissues were cut into 30-μm-thick sections.   The caudal brainstem tissues containing the NTS were cut into 25-μm-thick horizontal section at the position from interaural 2.2 to 1.6 mm (Mendelowitz et al., 1992).   Sections were blocked with 4% normal goat serum and incubated with the primary antibody (guinea pig anti-TRPV1, dilution 1:1000, Neuromics) for 2 hr at room temperature and overnight at 4°C.   Subsequently, sections were rinsed and incubated with the secondary antibody (Alexa Fluor-488 conjugated goat anti-guinea pig IgG, dilution 1:200, Molecular Probes) for 2 hr at room temperature.   Then, sections were rinsed and incubated with Alexa Fluor-594 conjugated IB$_4$ for 2 hr at room temperature.

Recording of Hemodynamics and Renal Sympathetic Nerve Activity (RSNA)

Before administration of anesthetics, the blood pressure of vehicle- and RTX-treated rats

was measured noninvasively using a tail cuff system (Model 29-SSP, IITC Life Science).

Three to four weeks after RTX or vehicle treatment, rats were anesthetized with urethane (800

mg/kg, i.p.) and α-chloralose (40 mg/kg, i.p.).   A midline incision was made in the neck, and

the trachea was cannulated for mechanical ventilation.   The left internal jugular vein and

femoral veins were exposed and cannulated with a PE50 catheter for administration of drugs.

The right femoral artery was cannulated to measure ABP with a pressure transducer (PT300,

Grass Instruments, Quincy, MA).   Heart rate (HR) was monitored by triggering from the

pulsatile ABP.

The left kidney and renal sympathetic nerve were exposed through a left retroperitoneal

flank incision.   A major branch of the renal nerve was isolated, carefully dissected from the

renal vasculature, insulated with mineral oil, and the central portion of the renal nerve placed on

a bipolar stainless steel recording electrode (Li et al., 2001; Zahner et al., 2003).   The nerve

signal was amplified with a direct current preamplifier (model P511, Grass Instruments) with the

filters set at 0.1 Hz and 3,000 Hz to remove low- and high-frequency interference.   The RSNA

was then monitored through an audio amplifier.   The RSNA and ABP were recorded using a

1401-PLUS analog-to-digital converter and the Spike2 system (Cambridge Electronic Design,

Cambridge, UK) and the recordings were stored on the hard disk of a computer.   Sympathetic

nerve signals were rectified and integrated offline with a 1-second time constant. Background

noise levels for RSNA were determined at the end of the experiment when nerve activity was

eliminated by injection of an overdose of sodium pentobarbital.   Background noise levels were

subtracted from all recordings to yield actual RSNA responses.   To quantify RSNA responses,

we calculated the percent changes of RSNA by taking the mean of the baseline control values as

100%.

Determination of Baroreflex Function

The baroreflex function was evaluated by measuring the reflex changes in RSNA and HR in response to decreases and increases in ABP induced by intravenous infusion of 50 μg/ml sodium nitroprusside (SNP) and 125 μg/ml phenylephrine (PE), respectively (Gao et al., 2004; McDowall et al., 2006). SNP and PE were administered via the jugular vein in successive ramped infusions at an initial rate of ~2.5 ml/hr, increased by 2.5 ml/hr every 30 s, to a maximum rate of 25 ml/hr by using a syringe pump (R99E, Razel, St. Albans, VT). The PE and SNA infusions were done separately with one drug administered after the blood pressure response of other drug had returned to baseline level, and the order of drugs was administered randomly. Infusions were ramped successively to achieve an approximately linear change in mean arterial pressure (MAP) at a rate of 1.5 mmHg/s. The maximum volume infused was 1.2 ml. Infusions were stopped before the maximum rate was reached if further changes in ABP no longer elicited changes in HR or RSNA or if MAP reached a minimum of 50 mmHg or a maximum of 200 mmHg. The recovery time for RSNA after PE-induced baroreflex responses in vehicle- and RTX-treated rats was determined by measuring the period of time elapsed between the peak increase in ABP and the return of RSNA (integrated voltage) to the baseline values after PE infusion.

In separate groups of rats, Iodo-RTX, a highly selective and potent TRPV1 antagonist (Wahl et al., 2001; Zahner et al., 2003), was intravenously injected (1 μmol/kg or 754 μg/kg) (Rigoni et al., 2003). The baroreflex function was determined 20-30 min after intravenous

injection of iodo-RTX. To verify if TRPV1 receptors were blocked after pretreatment with Iodo-RTX, capsaicin (10 μg/kg, iv) was used before and after Iodo-RTX pretreatment. The effect of capsaicin on RSNA, ABP, and HR were determined in vehicle-treated and iodo-RTX-treated rats.

Statistical Analysis

All data are expressed as means ± SEM. MAP data were acquired every 10 mmHg from the lowest pressure in response to SNP infusion to the highest pressure in response to PE infusion. A sigmoid logistic function was fit to the data using the nonlinear regression equation: $Y = A/\{1 + \exp[B(MAP - C)]\} + D$, where Y is RSNA or HR; A is the RSNA or HR range; B is the slope coefficient; C is the MAP at the midpoint of the RSNA or HR range (which is also the point of maximum gain); and D is the minimum RSNA or HR (Kent et al., 1972; Gao et al., 2004). The baroreflex curves were differentiated to determine the gain of the HR and RSNA components of the baroreflex across the MAP range (Kent et al., 1972; Gao et al., 2004). The maximum gain was determined by taking the first derivative of the baroreflex curve described by the logistic equation. Differences between the treatment groups were compared by using ANOVA with Bonferroni's *post hoc* test. $P < 0.05$ was considered statistically significant.

Results

RTX Treatment Diminishes Thermal Nociception

To confirm that RTX treatment depletes TRPV1-expressing somatic afferent neurons, we examined thermal sensitivity by testing the paw withdrawal latency in response to a noxious heat stimulus in vehicle- and RTX-treated rats. Before vehicle or RTX treatment, the mean paw withdrawal latency was 6.28 ± 0.29 and 6.37 ± 0.32 s in the vehicle- and RTX-treated group, respectively. Three weeks after treatment, the mean paw withdrawal latency (6.53 ± 0.46 s) did not significantly change in vehicle-treated rats. However, in the RTX-treated rats, the mean paw withdrawal latency significantly increased and nearly reached the 30-s cutoff (6.37 ± 0.32 vs. 27.89 ± 3.5 s, $P < 0.05$).

TRPV1 Is Expressed on Afferent Fibers in the Ascending Aorta and Aortic Arch

We determined the presence of TRPV1 in afferent nerves and terminals surrounding the ascending aorta and aortic arch. TRPV1 immunoreactivities were densely expressed in helical loop formations in the adventitia and tunica media of the ascending aorta and aortic arch in the vehicle-treated rats (Fig. 1, A-C). The TRPV1-immunoreactive puncta and tortuous fibers formed a nerve plexus and arborized along the adventitia of the aorta (Figs. 1 and 2).

To examine if TRPV1 is expressed on myelinated nerve fibers, NF200 was used as a marker for myelinated fibers. Although some TRPV1-immunoreactive nerve fibers were not co-localized with NF200, many nerve bundles contained both TRPV1- and NF200-immunoreactivities (Fig. 2A). In RTX-treated rats, TRPV1-immunoreactive fibers

were completely eliminated in the region of the ascending aorta and aortic arch (Figs. 1D and 2B).   However, some NF200-immunoreactive nerves were still visible near the adventitia of the aorta and aortic arch.

TRPV1 Is Expressed in NG Neurons and Afferent Fibers in the Solitary Tract

Next, we determined TRPV1-immunoreactivities in the NG and DRG in vehicle- and RTX-treated rats. IB_4 was used as a marker for small- and medium-sized neurons (Bailey et al., 2002; Wu et al., 2004).   In vehicle-treated rats, TRPV1- and IB_4-positive neurons were co-localized in the majority of neurons with a diameter of 15-40 μm in the NG (Fig. 3A) and DRG (Fig. 3B).   But some of the TRPV1-immunoreactive neurons were not co-localized with IB_4.   In RTX-treated rats, TRPV1-expressing neurons were largely eliminated in both the NG and DRG (Fig. 3, A and B).   However, a few IB_4-positive neurons were still presented in the NG and DRG.

We then examined the presence of TRPV1-immunoreactive afferent fibers near the medial region of the NTS.   In vehicle-treated rats, TRPV1-immunoreactive nerve fibers and puncta were present in the solitary tract (Fig. 4A).   Most TRPV1-immunoreactive fibers along the solitary tract were co-localized with IB_4 and terminated in the medial region of the NTS.   In RTX-treated rats, TRPV1-immunoreactive afferent fibers in the solitary tract were completely eliminated.   Also, RTX treatment largely reduced IB_4-positive afferent fibers in the solitary tract but had little effect on TRPV1-expressing neurons in the brainstem (Fig. 4B).

Baroreflex Control of RSNA and HR by TRPV1-expressing Neurons

We subsequently studied the functional significance of TRPV1-expressing baroreceptive neurons in the baroreflex. The baroreflex curves for RSNA and HR were generated by intravenous infusion of PE and SNP in 15 vehicle- and 12 RTX-treated rats. The systolic blood pressure, which was measured while rats were conscious with the tail cuff system, was not significantly different between vehicle- and RTX-treated rats (136.8 ± 3.1 vs. 142.5 ± 3.5 mmHg). In vehicle-treated rats, PE-induced increases in ABP resulted in a marked inhibition of RSNA and bradycardia (Fig. 5), while SNP-induced decreases in ABP led to a large increase in RSNA and tachycardia. In the RTX treatment group, the baroreflex function curves of MAP-RSNA and MAP-HR were shifted upwards to higher heart rate and sympathetic nerve activity in the high blood pressure range (> 120 mmHg; Fig. 5, C and D). The maximum gain of the baroreflex curve was significantly decreased in RTX-treated compared to vehicle-treated rats. However, the maximum increases in RSNA and HR induced by a decrease in ABP were not altered by RTX treatment (Fig. 5, C and D). The RSNA measured at the peak increase in ABP was significantly higher in RTX-treated than in vehicle-treated rats (49.6 ± 3.54% vs. 19.95 ± 0.68%). The HR value after maximum increase in ABP was also significantly higher in RTX-treated than in vehicle-treated rats (296.7 ± 8.8 vs. 270.5 ± 8.4 bpm). Although the magnitude of induced BP increase was not significantly different between vehicle-treated and RTX-treated rats, the recovery time for RSNA in RTX-treated rats was significantly longer than that in vehicle-treated rats (156 ± 23 vs. 16 ± 5 s).

Role of TRPV1 Receptors in Baroreflex Control of RSNA and HR

To further determine if TRPV1 receptors play a role in the baroreflex function, we tested

whether blockade of TRPV1 receptors affected the baroreflex responses. First, we used capsaicin to verify that TRPV1 receptors were blocked by pretreatment with iodo-RTX, a highly selective and potent TRPV1 receptor antagonist (Wahl et al., 2001; Zahner et al., 2003). Intravenous injection of capsaicin (10 μg/kg) caused a triphasic change in ABP, initially it acted as a transient depressor followed then as a brief pressor, finally causing a prolonged decrease in blood pressure. Also, capsaicin decreased RSNA and HR (n = 6, Fig. 6). Intravenous injection of 1 μmol/kg (i.e., 754 μg/kg) of iodo-RTX alone did not significantly change the baseline RSNA and ABP. This dose of iodo-RTX was selected from a previous study using systemic treatment of iodo-RTX (Rigoni et al., 2003). After pretreatment with iodo-RTX, subsequent capsaicin injection caused only a brief fluctuation in HR (n = 8, Fig. 6).

The baroreflex function was determined 20-30 min after intravenous treatment with iodo-RTX (1 μmol/kg, n = 7) or the vehicle (n = 6). In the iodo-RTX treatment, the baroreflex function curves of MAP-RSNA and MAP-HR were shifted upwards in the high blood pressure range (Fig. 7). The maximum gain of the baroreflex curve was also significantly decreased in iodo-RTX-treated compared to vehicle-treated rats. The remaining RSNA at the peak increase in ABP was significantly higher in iodo-RTX-treated than in vehicle-treated rats ($50.3 \pm 1.4\%$ vs. $21.5 \pm 2.8\%$). Also, the HR value measured at the maximum increase in ABP was significantly higher in iodo-RTX-treated than in vehicle-treated rats (307.1 ± 9.6 vs. 274.8 ± 10.8 bpm). However, treatment with iodo-RTX did not significantly alter the responses of RSNA and HR to SNP-induced decrease in ABP. Furthermore, the recovery time for RSNA in iodo-RTX-treated rats was significantly longer than that in vehicle-treated rats (121 ± 31vs. 20 ± 6 s).

Discussion

Although it has been recognized for several decades that the baroreflex has an important physiological function in cardiovascular homeostasis, the phenotypes of baroreceptive neurons and the sensory molecules involved in detection of blood pressure changes are still poorly understood. Our study provides new evidence that the ascending aorta and aortic arch are densely innervated by TRPV1-expressing afferent nerve endings. Previously published immunohistochemical and *in situ* hybridization data suggest that TRPV1 is present in the NG neurons (Helliwell et al., 1998; Mezey et al., 2000; Patterson et al., 2003). Our immunocytochemical analysis revealed that TRPV1 receptors were expressed throughout the entire baroreceptive afferent pathway, which includes the nerve terminals innervating the ascending aorta, NG neurons, and afferent nerves in the solitary tract. Moreover, our study provide new histologic evidence of the complex structures of TRPV1-expressing afferent terminals surrounding the aortic arch and ascending aorta. Furthermore, our study demonstrated that RTX treatment depleted TRPV1-expressing afferent fibers and terminals along the baroreceptive afferent pathway, indicating that the baroreceptive afferent pathway is innervated along its entirety by TRPV1.

TRPV1 receptors are best known for their function in sensing noxious heat in the skin (Caterina et al., 1997). Thermal sensitivity was profoundly diminished in our RTX-treated rats, suggesting that RTX treatment resulted in a substantial deletion of TRPV1-expressing cutaneous afferent fibers. A recent study reported that TRPV1 is expressed in most unmyelinated C-fibers and in about 30% of lightly myelinated fibers in the somatic nerve fibers (Ma, 2002).

In this study, we found that the majority of TRPV1-immunoreactive fibers and neurons were co-localized with IB$_4$-positive unmyelinated nerves and NG neurons. However, some afferent fibers surrounding the ascending aorta were immunoreactive to both TRPV1 and NF200, suggesting that TRPV1 is also present in a small number of myelinated fibers. Therefore, we can conclude that RTX treatment not only eliminated unmyelinated nerve fibers but also potentially ablated a subpopulation of myelinated baroreceptive fibers. Notably, RTX treatment had little effect on TRPV1-expressing neurons in the brainstem. This selective peripheral effect of RTX was likely due to the failure of RTX to cross the blood-brain barrier or the high density of TRPV1 in primary afferent neurons (Chen and Pan, 2006; Zhou et al., 2009).

An important finding of our study is that TRPV1-expressing baroreceptors are involved in sensing the elevation in blood pressure. We found that the baroreflex control of RSNA and HR in the high blood pressure range was profoundly impaired in RTX-treated rats. Thus, TRPV1-expressing baroreceptive afferents are important for the feedback control of blood pressure stability. In general, Aδ-fiber baroreceptors have lower pressure thresholds, higher mean discharge rates, and higher sensitivities than C-fiber baroreceptors (Coleridge et al., 1973; Thoren et al., 1977; Seagard et al., 1990; Kunze and Andresen, 1991; Thoren et al., 1999). These characteristic differences between Aδ-and C-fibers support the notion that Aδ-fibers are primarily important for baroreflex responses at normal and low blood pressure ranges, whereas C-fibers are mainly involved in baroreceptive regulation in the high blood pressure range. The differences in the dynamic and static characteristics of unmyelinated and myelinated fibers may result from the differences in the way that their nerve endings come in contact with the aortic wall. For instance, the nerve endings of myelinated fibers appear to be tightly coupled to the

vessel wall, which may explain their high sensitivity to changes in ABP (Bock and Gorgas, 1976). Importantly, the baroreceptive nerves have a higher number of C-fibers than Aδ-fibers (Brown et al., 1976; Krauhs, 1979), suggesting that C-fiber baroreceptors likely have a critical role in the blood pressure control. In this study, we found that RSNA and HR at the maximum increase in ABP remained significantly higher in RTX-treated than in vehicle-treated rats. Also, the maximum gain of the baroreflex function curve was significantly decreased in RTX-treated rats. These data suggest that TRPV1-expressing baroreceptors play an important role in the feedback control of sympathetic outflow in the high blood pressure range. We observed that the baseline blood pressure was not significantly different between RTX- and vehicle-treated rats. It is possible that the remaining non-TRPV1-expressing Aδ-fibers may compensate for the loss of TRPV1-expressing baroreceptive afferent fibers in RTX-treated animals.

Another salient finding of our study is that TRPV1 receptors in baroreceptor nerve endings function as mechanoreceptors in sensing increases in ABP. In our study, we found that systemic treatment with iodo-RTX, a highly specific TRPV1 blocker, profoundly impaired the baroreflex function in the high blood pressure range. Our findings are consistent with those from recent studies suggesting that TRPV1 receptors present in the visceral organs, including the gastrointestinal tract and urinary bladder (Birder et al., 2002; Rong et al., 2004; Jones et al., 2005), can detect mechanical changes in the tissue. Also, we previously showed that TRPV1-expressing afferent nerves on the epicardial surface are capable of responding to myocardial ischemia (Zahner et al., 2003; Pan and Chen, 2004). We found that reflex responses to SNP was preserved in RTX-treated rats and after blocking TRPV1, suggesting that

TRPV1-expressing and non-TRPV1-expressing afferent nerves are differentially involved in baroreflex regulation. Our findings provide further evidence for the new emerging physiological functions of TRPV1 in the visceral organs and tissues.

We found that the recovery times for RSNA after PE-induced increases in ABP were much longer in RTX- and iodo-RTX-treated rats than in vehicle-treated rats. The exact reasons for the prolonged inhibition of RSNA after baroreceptor activation in rats lacking TRPV1-expressing baroreceptors are not clear. It has been shown that high-frequency stimulation of the aortic depressor nerve causes a prolonged depressor response after nerve stimulation ceases, probably because of the enhanced activation of NTS neurons by stimulation of A-fibers (Tang and Dworkin, 2007). It is possible that baroreceptor activation may produce an extended stimulation of NTS neurons through non-TRPV1-expressing baroreceptive inputs leading to a prolonged inhibition of RSNA. The synaptic plasticity in the NTS after the loss of TRPV1-expressing baroreceptive afferents warrants further investigation. Because RTX does not cross the blood-brain barrier, RTX treatment has no effect on intrinsic TRPV1-expressing neurons in the central nervous system (Chen and Pan, 2006; Zhou et al., 2009). Also, there is no evidence showing that TRPV1 receptors are expressed on sympathetic neurons. We have shown that centrally-induced sympathetic outflow is not altered in RTX-treated rats (Zahner et al., 2003). Nevertheless, because TRPV1 receptors are present in the areas of sensory nerves in the arterial vascular wall, it cannot be excluded that the altered baroreflex curve by RTX/iodo-RTX treatments may represent, to some extent, lack of afferent signals from more than the aortic and carotid baroreceptor area.

In summary, our study provides important histologic and functional evidence about the

new role of TRPV1 receptors and TRPV1-expressing baroreceptive neurons in the autonomic

control of cardiovascular function.   Because a normal baroreflex function is essential to the

short-term and long-term stability of blood pressure, the dysfunction of TRPV1 receptors or

TRPV1-expressing baroreceptive neurons could lead to impaired cardiovascular regulation in

disease conditions such as congestive heart failure and hypertension.

References

Averill S, McMahon SB, Clary DO, Reichardt LF and Priestley JV (1995) Immunocytochemical localization of trkA receptors in chemically identified subgroups of adult rat sensory neurons. *Eur J Neurosci* **7**:1484-1494.

Bailey TW, Jin YH, Doyle MW and Andresen MC (2002) Vanilloid-sensitive afferents activate neurons with prominent A-type potassium currents in nucleus tractus solitarius. *J Neurosci* **22**:8230-8237.

Bennett DL, Michael GJ, Ramachandran N, Munson JB, Averill S, Yan Q, McMahon SB and Priestley JV (1998) A distinct subgroup of small DRG cells express GDNF receptor components and GDNF is protective for these neurons after nerve injury. *J Neurosci* **18**:3059-3072.

Birder LA, Nakamura Y, Kiss S, Nealen ML, Barrick S, Kanai AJ, Wang E, Ruiz G, De Groat WC, Apodaca G, Watkins S and Caterina MJ (2002) Altered urinary bladder function in mice lacking the vanilloid receptor TRPV1. *Nat Neurosci* **5**:856-860.

Bock P and Gorgas K (1976) Fine structure of baroreceptor terminals in the carotid sinus of guinea pigs and mice. *Cell Tissue Res* **170**:95-112.

Bradbury EJ, Burnstock G and McMahon SB (1998) The expression of P2X3 purinoreceptors in sensory neurons: effects of axotomy and glial-derived neurotrophic factor. *Mol Cell Neurosci* **12**:256-268.

Brown AM, Saum WR and Tuley FH (1976) A comparison of aortic baroreceptor discharge in normotensive and spontaneously hypertensive rats. *Circ Res* **39**:488-496.

22

Caterina MJ, Rosen TA, Tominaga M, Brake AJ and Julius D (1999) A capsaicin-receptor
homologue with a high threshold for noxious heat. *Nature* **398**:436-441.

Caterina MJ, Schumacher MA, Tominaga M, Rosen TA, Levine JD and Julius D (1997) The
capsaicin receptor: a heat-activated ion channel in the pain pathway. *Nature*
389:816-824.

Chen SR and Pan HL (2006) Loss of TRPV1-expressing sensory neurons reduces spinal mu
opioid receptors but paradoxically potentiates opioid analgesia. *J Neurophysiol*
95:3086-3096.

Coleridge HM, Coleridge JC, Dangel A, Kidd C, Luck JC and Sleight P (1973) Impulses in
slowly conducting vagal fibers from afferent endings in the veins, atria, and arteries of
dogs and cats. *Circ Res* **33**:87-97.

Doyle MW, Bailey TW, Jin YH and Andresen MC (2002) Vanilloid receptors presynaptically
modulate cranial visceral afferent synaptic transmission in nucleus tractus solitarius. *J
Neurosci* **22**:8222-8229.

Gao L, Zhu Z, Zucker IH and Wang W (2004) Cardiac sympathetic afferent stimulation impairs
baroreflex control of renal sympathetic nerve activity in rats. *Am J Physiol Heart Circ
Physiol* **286**:H1706-1711.

Guo A, Vulchanova L, Wang J, Li X and Elde R (1999) Immunocytochemical localization of the
vanilloid receptor 1 (VR1): relationship to neuropeptides, the P2X3 purinoceptor and
IB4 binding sites. *Eur J Neurosci* **11**:946-958.

Helliwell RJ, McLatchie LM, Clarke M, Winter J, Bevan S and McIntyre P (1998) Capsaicin
sensitivity is associated with the expression of the vanilloid (capsaicin) receptor (VR1)

mRNA in adult rat sensory ganglia. *Neurosci Lett* **250**:177-180.

Jin YH, Bailey TW, Li BY, Schild JH and Andresen MC (2004) Purinergic and vanilloid receptor activation releases glutamate from separate cranial afferent terminals in nucleus tractus solitarius. *J Neurosci* **24**:4709-4717.

Jones RC, 3rd, Xu L and Gebhart GF (2005) The mechanosensitivity of mouse colon afferent fibers and their sensitization by inflammatory mediators require transient receptor potential vanilloid 1 and acid-sensing ion channel 3. *J Neurosci* **25**:10981-10989.

Kent BB, Drane JW, Blumenstein B and Manning JW (1972) A mathematical model to assess changes in the baroreceptor reflex. *Cardiology* **57**:295-310.

Krauhs JM (1979) Structure of rat aortic baroreceptors and their relationship to connective tissue. *J Neurocytol* **8**:401-414.

Kunze DL and Andresen MC (1991) Arterial baroreceptors: excitation and modulation., in *Reflex Control of Circulation* (Zucker IH and Gilmore JP eds) pp 141-166, CRC,, Boca Raton, FL.

Li DP, Averill DB and Pan HL (2001) Differential roles for glutamate receptor subtypes within commissural NTS in cardiac-sympathetic reflex. *Am J Physiol Regul Integr Comp Physiol* **281**:R935-943.

Ma QP (2002) Expression of capsaicin receptor (VR1) by myelinated primary afferent neurons in rats. *Neurosci Lett* **319**:87-90.

McDowall LM, Horiuchi J, Killinger S and Dampney RA (2006) Modulation of the baroreceptor reflex by the dorsomedial hypothalamic nucleus and perifornical area. *Am J Physiol Regul Integr Comp Physiol* **290**:R1020-1026.

McMahon SB, Armanini MP, Ling LH and Phillips HS (1994) Expression and coexpression of Trk receptors in subpopulations of adult primary sensory neurons projecting to identified peripheral targets. *Neuron* **12**:1161-1171.

Mendelowitz D, Yang M, Andresen MC and Kunze DL (1992) Localization and retention in vitro of fluorescently labeled aortic baroreceptor terminals on neurons from the nucleus tractus solitarius. *Brain Res* **581**:339-343.

Mezey E, Toth ZE, Cortright DN, Arzubi MK, Krause JE, Elde R, Guo A, Blumberg PM and Szallasi A (2000) Distribution of mRNA for vanilloid receptor subtype 1 (VR1), and VR1-like immunoreactivity, in the central nervous system of the rat and human. *Proc Natl Acad Sci U S A* **97**:3655-3660.

Michael GJ and Priestley JV (1999) Differential expression of the mRNA for the vanilloid receptor subtype 1 in cells of the adult rat dorsal root and nodose ganglia and its downregulation by axotomy. *J Neurosci* **19**:1844-1854.

Pan HL and Chen SR (2004) Sensing tissue ischemia: another new function for capsaicin receptors? *Circulation* **110**:1826-1831.

Pan HL, Khan GM, Alloway KD and Chen SR (2003) Resiniferatoxin induces paradoxical changes in thermal and mechanical sensitivities in rats: mechanism of action. *J Neurosci* **23**:2911-2919.

Patterson LM, Zheng H, Ward SM and Berthoud HR (2003) Vanilloid receptor (VR1) expression in vagal afferent neurons innervating the gastrointestinal tract. *Cell Tissue Res* **311**:277-287.

Perry MJ, Lawson SN and Robertson J (1991) Neurofilament immunoreactivity in populations

of rat primary afferent neurons: a quantitative study of phosphorylated and non-phosphorylated subunits. *J Neurocytol* **20**:746-758.

Rigoni M, Trevisani M, Gazzieri D, Nadaletto R, Tognetto M, Creminon C, Davis JB, Campi B, Amadesi S, Geppetti P and Harrison S (2003) Neurogenic responses mediated by vanilloid receptor-1 (TRPV1) are blocked by the high affinity antagonist, iodo-resiniferatoxin. *Br J Pharmacol* **138**:977-985.

Rong W, Hillsley K, Davis JB, Hicks G, Winchester WJ and Grundy D (2004) Jejunal afferent nerve sensitivity in wild-type and TRPV1 knockout mice. *J Physiol* **560**:867-881.

Seagard JL, Hopp FA, Drummond HA and Van Wynsberghe DM (1993) Selective contribution of two types of carotid sinus baroreceptors to the control of blood pressure. *Circ Res* **72**:1011-1022.

Seagard JL, van Brederode JF, Dean C, Hopp FA, Gallenberg LA and Kampine JP (1990) Firing characteristics of single-fiber carotid sinus baroreceptors. *Circ Res* **66**:1499-1509.

Tang X and Dworkin BR (2007) Baroreflexes of the rat. V. Tetanus-induced potentiation of ADN A-fiber responses at the NTS. *Am J Physiol Regul Integr Comp Physiol* **293**:R2254-2259.

Thoren P, Munch PA and Brown AM (1999) Mechanisms for activation of aortic baroreceptor C-fibres in rabbits and rats. *Acta Physiol Scand* **166**:167-174.

Thoren P, Saum WR and Brown AM (1977) Characteristics of rat aortic baroreceptors with nonmedullated afferent nerve fibers. *Circ Res* **40**:231-237.

Tranum-Jensen J (1975) The ultrastructure of the sensory end-organs (baroreceptors) in the atrial endocardium of young mini-pigs. *J Anat* **119**:255-275.

Wahl P, Foged C, Tullin S and Thomsen C (2001) Iodo-resiniferatoxin, a new potent vanilloid receptor antagonist. *Mol Pharmacol* **59**:9-15.

Wang H, Rivero-Melian C, Robertson B and Grant G (1994) Transganglionic transport and binding of the isolectin B4 from Griffonia simplicifolia I in rat primary sensory neurons. *Neuroscience* **62**:539-551.

Wu ZZ, Chen SR and Pan HL (2004) Differential sensitivity of N- and P/Q-type Ca2+ channel currents to a mu opioid in isolectin B4-positive and -negative dorsal root ganglion neurons. *J Pharmacol Exp Ther* **311**:939-947.

Zahner MR, Li DP, Chen SR and Pan HL (2003) Cardiac vanilloid receptor 1-expressing afferent nerves and their role in the cardiogenic sympathetic reflex in rats. *J Physiol* **551**:515-523.

Zhou HY, Chen SR, Chen H and Pan HL (2009) The glutamatergic nature of TRPV1-expressing neurons in the spinal dorsal horn. *J Neurochem* **108**:305-318.

Footnotes

Legends for Figures

Figure 1. Confocal images show TRPV1-expressing nerve fibers and terminals in the ascending aorta and aortic arch. A - C, TRPV1-immunoreactive nerve fibers and terminals were present in the adventitia of the ascending aorta and aortic arch in vehicle-treated rats. D, TRPV1-immunoreactive nerve fibers were eliminated in the adventitia of the ascending aorta of in one RTX-treated rat. Maximum projection images were obtained from the Z-stack confocal images.

Figure 2. Confocal images show the spatial relationship between TRPV1- and NF200-immunoreactive nerve fibers in the ascending aorta and aortic arch. A, TRPV1- and NF200-immunoreactive nerve fibers and terminals were present in the adventitia of the ascending aorta and aortic arch of one vehicle-treated rat. Co-localization of TRPV1-and NF200-immunoreactivities is indicated in yellow when two images are digitally merged. B, Nerve fibers immunoreactive to both TRPV1 and NF200 were eliminated in the ascending aorta of one RTX-treated rat. Maximum projection images were obtained from the Z-stack confocal images.

Figure 3. Confocal images depict the presence of TRPV1 and IB$_4$ positive neurons in the NG and DRG. A, TRPV1- and IB$_4$-positive neurons in the NG of one vehicle- and one RTX-treated rat. TRPV1 and IB$_4$ are present in the majority of NG neurons. RTX treatment eliminated all TRPV1-immunoreactive neurons and most IB$_4$-positive neurons in the NG. B,

TRPV1- and IB$_4$-positive neurons in the DRG of one vehicle- and one RTX-treated rat. RTX treatment eliminated all TRPV1-expressing neurons and most IB$_4$-positive neurons in the DRG. All images are single confocal optical sections.

Figure 4. Confocal images show the presence of TRPV1- and IB$_4$-positive afferent fibers in the solitary tract. A, Low- and high-magnification confocal images show the presence of TRPV1- and IB$_4$-positive afferent fibers in the solitary tract (ST) in a vehicle-treated rat. The majority of TRPV1-immunoreactive fibers are co-localized with IB$_4$ in the ST and terminate in the medial region of the nucleus tractus solitarius (mNTS). B, Low- and high-magnification confocal images show diminished TRPV1- and IB$_4$-positive nerve fibers in the ST of one RTX-treated rat. All images are single confocal optical sections.

Figure 5. Baroreflex functions in vehicle- and RTX-treated rats. A and B, Original recordings depict the changes in RSNA and HR in response to ABP changes induced by intravenous injection of phenylephrine (PE) in one vehicle- and one RTX-treated rat. C and D, Baroreflex function curves derived from reflex changes in RSNA and HR in 15 vehicle- and 12 RTX-treated rats. *Inset,* gain of the mean baroreflex curves. The maximum gain values in C in vehicle- and RTX-treated rats are -1.8 ± 0.3 and -1.1 ± 0.2 %.mmHg^{-1} ($P < 0.05$), respectively. The maximum gain values in D in vehicle- and RTX-treated rats are -1.2 ± 0.1 and -0.8 ± 0.2 bpm.mmHg^{-1} ($P < 0.05$), respectively.

**Figure 6. Iodo-RTX blocks capsaicin-induced changes in the blood pressure, RSNA, and**

HR. A, original records show the effect of capsaicin (10 μg/kg, iv) on ABP, RSNA, and HR in one rat. B, Effect of capsaicin (10 μg/kg, iv) on ABP, RSNA, and HR was diminished after pretreatment with iodo-RTX (1 μmol/kg, iv) in one rat. C, Group data show the effect of capsaicin (10 μg/kg, iv) on changes in MAP, RSNA, and HR in rats pretreated with the vehicle (n = 6) or iodo-RTX (n = 8). * P < 0.05 compared with the respective control.

Figure 7. Effect of blocking TRPV1 on the baroreflex function. A and B, Original recordings show reflex changes in RSNA and HR in response to ABP increases induced by intravenous injection of phenylephrine (PE) in one vehicle and one iodo-RTX (1 μmol/kg, iv)-treated rat. C and D, Baroreflex function curves derived from reflex changes in RSNA and HR in 6 vehicle- and 7 iodo-RTX-treated rats. *Inset,* gain of the mean baroreflex curves. The maximum gain values in C in vehicle- and iodo-RTX-treated rats are -1.7 ± 0.3 and -1.1 ± 0.2 %.mmHg^{-1} (P < 0.05), respectively. The maximum gain values in D in vehicle- and iodo-RTX-treated rats are -1.2 ± 0.2 and -0.7 ± 0.1 bpm.mmHg^{-1} (P < 0.05), respectively.
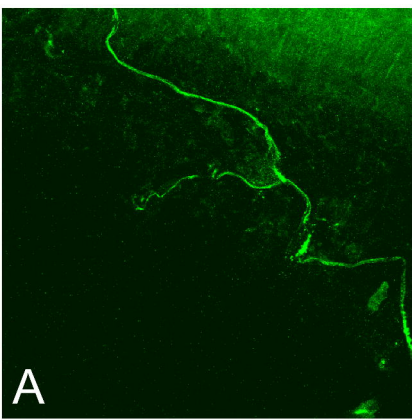
Fig. 1

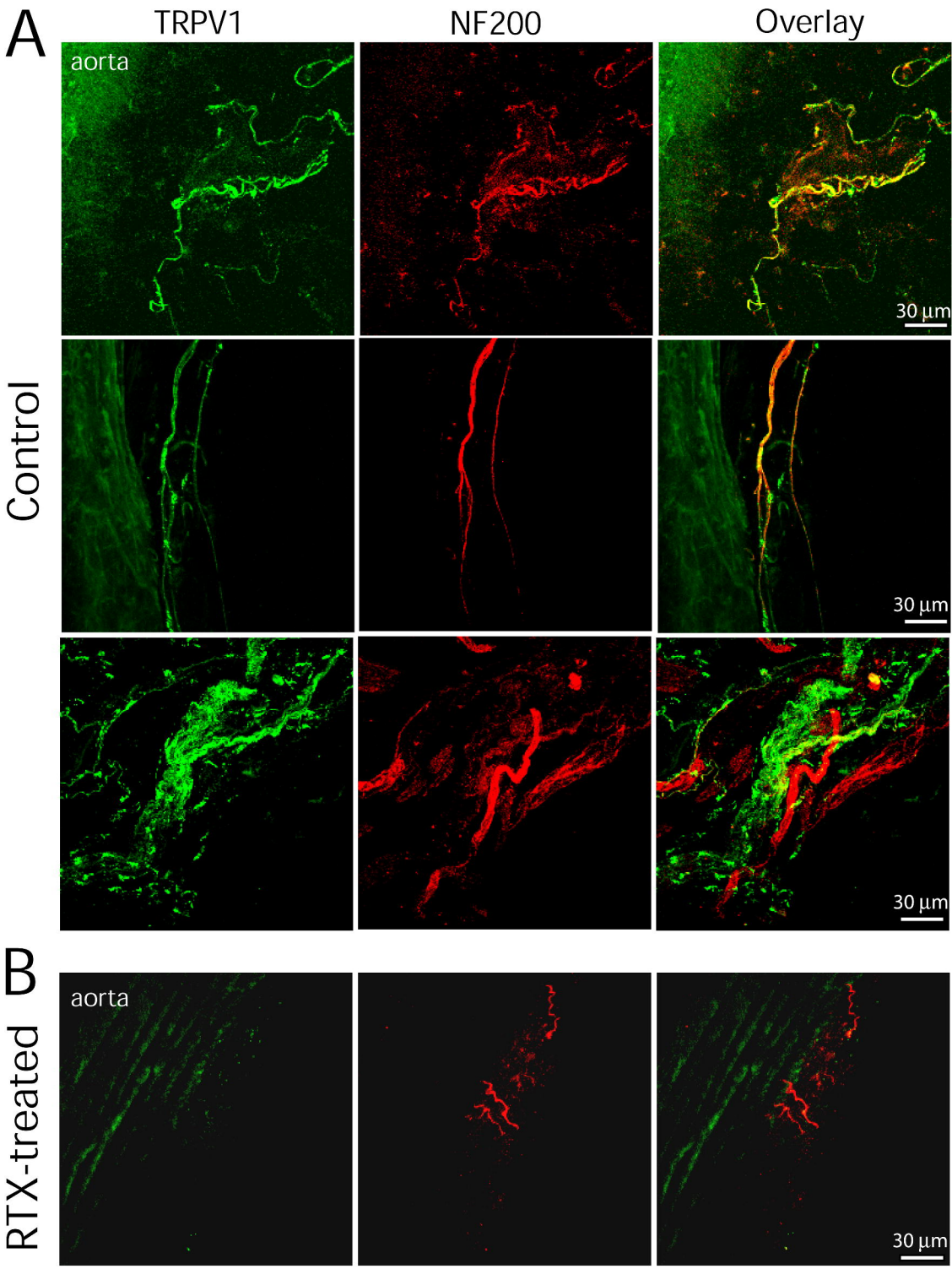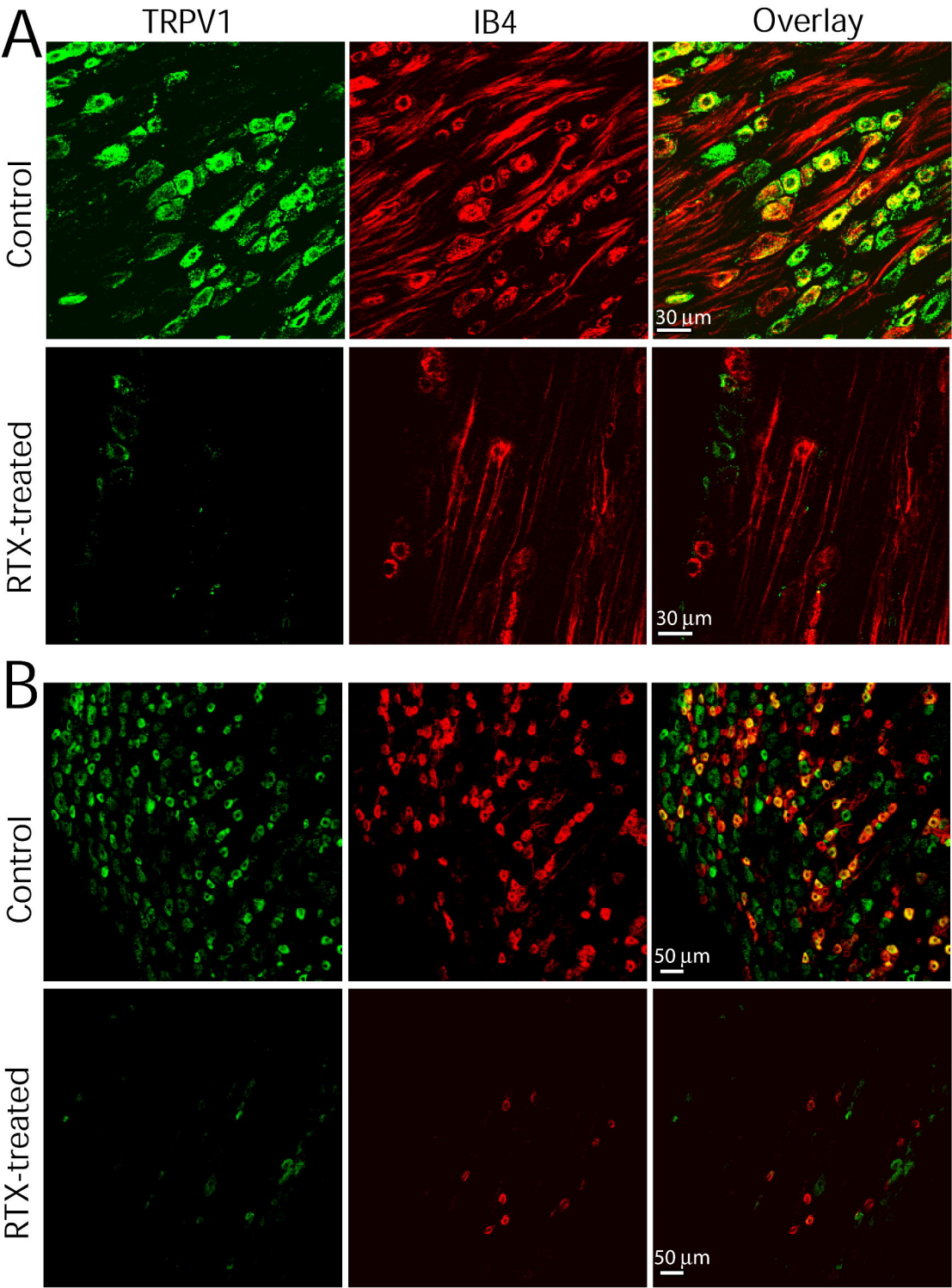| | TRPV1 | NF200 | Overlay |

A — Control — aorta

B — RTX-treated — aorta
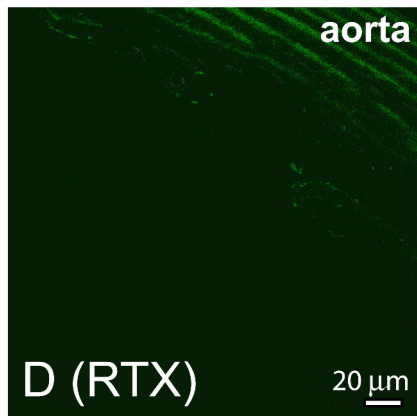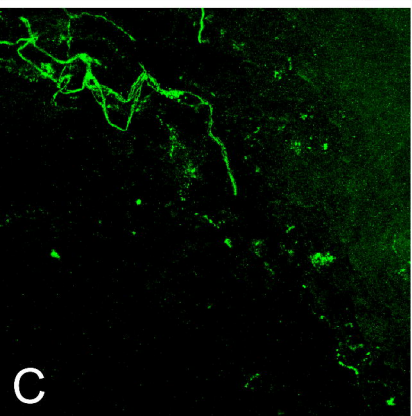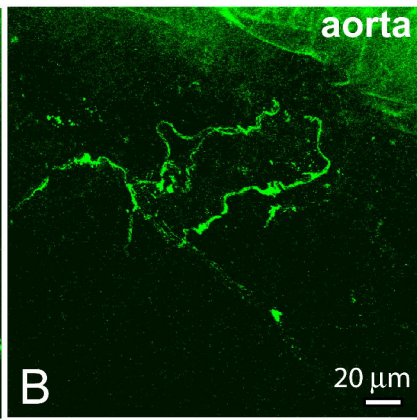
Fig. 2

Fig. 3
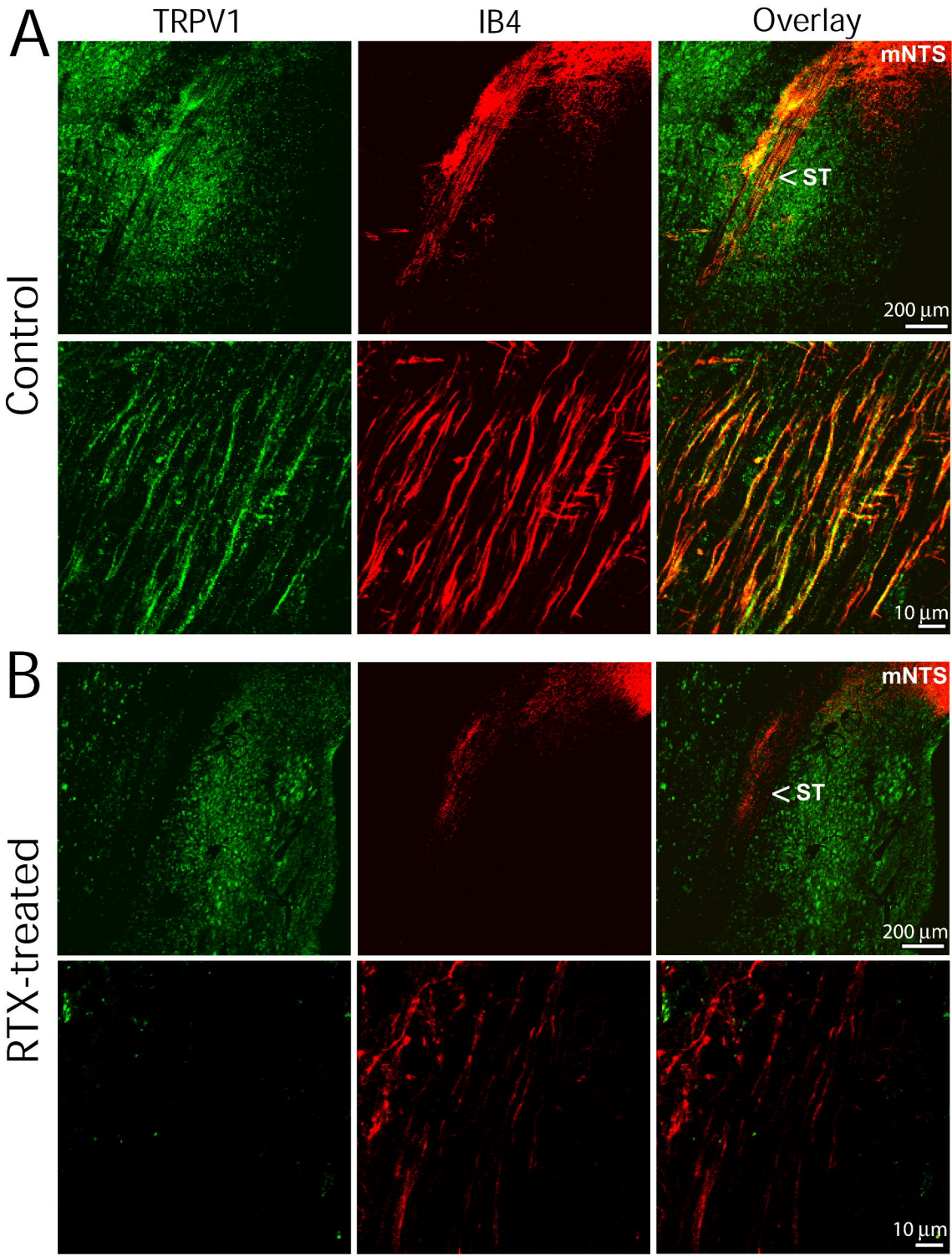
Fig. 4
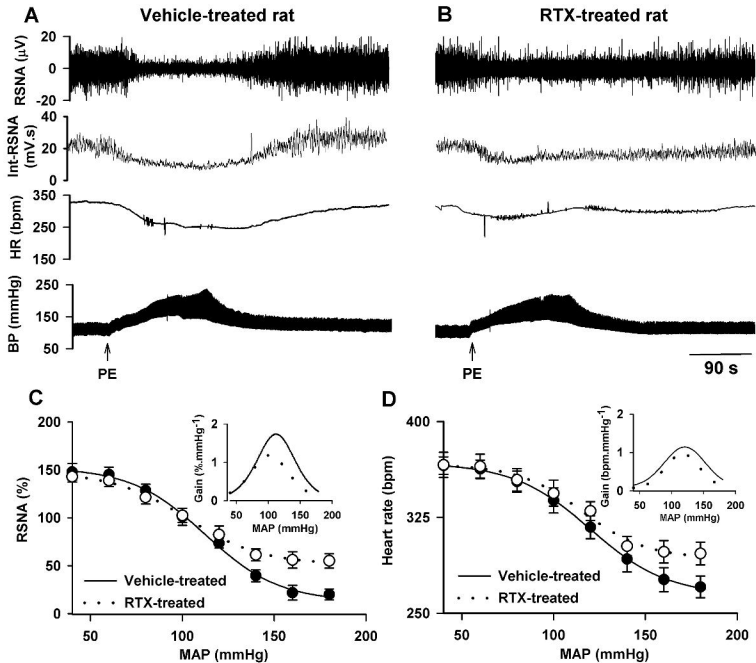
Figure 5

Figure 6

Figure 7